Taming the Yukawa potential singularity: improved evaluation of bound states and resonance energies

2008 J. Phys. A: Math. Theor. 41 032001

(http://iopscience.iop.org/1751-8121/41/3/032001)

IOP FTC
IOP Publishing Journal of Physics A: Mathematical and Theoretical

J. Phys. A: Math. Theor. **41** (2008) 032001 (9pp) doi:10.1088/1751-8113/41/3/032001

FAST TRACK COMMUNICATION

Taming the Yukawa potential singularity: improved evaluation of bound states and resonance energies

A D Alhaidari[1], H Bahlouli[2] and M S Abdelmonem[2]

[1] Shura Council, Riyadh 11212, Saudi Arabia
[2] Physics Department, King Fahd University of Petroleum & Minerals, Dhahran 31261, Saudi Arabia

E-mail: haidari@mailaps.org

Received 18 October 2007, in final form 4 December 2007
Published 4 January 2008
Online at stacks.iop.org/JPhysA/41/032001

Abstract
Using the tools of the J-matrix method, we absorb the $1/r$ singularity of the Yukawa potential in the reference Hamiltonian, which is handled analytically. The remaining part, which is bound and regular everywhere, is treated by an efficient numerical scheme in a suitable basis using the Gauss quadrature approximation. Analysis of resonance energies and bound states spectrum is performed using the complex scaling method, where we show their trajectories in the complex energy plane and construct a video showing how bound states cross over into resonance states by varying the potential parameters.

PACS numbers: 03.65.Ge, 34.20.Cf, 03.65.Nk, 34.20.Gj

M This article features online multimedia enhancements

(Some figures in this article are in colour only in the electronic version)

The Yukawa potential [1] is used in various areas of physics to model singular but short-range interactions. In high energy physics, for example, it is used to model the interaction of hadrons in short-range gauge theories where coupling is mediated by the exchange of a massive scalar meson [1, 2]. In atomic and molecular physics, it represents a screened Coulomb potential due to the cloud of electronic charges around the nucleus, which could be treated in the Thomas–Fermi approximation that leads to [3]

$$V(r) = -\frac{A}{r}\,\mathrm{e}^{-\mu r}, \tag{1}$$

where μ is the screening parameter and A is the potential strength. This potential also describes the shielding effect of ions embedded in plasmas where it is called the Debye–Hückel potential [4]. It has also been used to describe the interaction between charged particles in plasmas, solids and colloidal suspensions [5]. The number of bound states of the Yukawa potential is always finite. However, due to the delicate nature of the resonances in the Yukawa

potential, this subject did not receive adequate attention in the literature [6]. The solution of the Schrödinger equation for this potential has been investigated extensively in the past using various numerical and perturbative approaches since exact analytical solutions are not possible [7]. Despite the short-range behavior of the potential due to the decaying exponential factor $e^{-\mu r}$, the r^{-1} singularity at the origin makes the task of obtaining accurate or even meaningful solutions a non-trivial and sometimes formidable task. Most of the perturbative and variational calculations found in the literature suffer from the limited accuracy when considering a wider range of potential parameters. Our approach constitutes a significant contribution in this regard. It is inspired by the J-matrix method [8] that handles this particular singularity not just accurately but, in fact, exactly leaving the remaining non-singular and finite part to be easily treated numerically to the desired accuracy.

The J-matrix method is an algebraic method for extracting resonance and bound states information using computational tools devised entirely in square-integrable bases. The total Hamiltonian is a sum two parts: a reference Hamiltonian H_0 and the remaining terms which are combined into an effective potential $U(r)$. The reference Hamiltonian is treated analytically and, thus, its contribution will be accounted for in full. As such, it must belong to the class of exactly solvable problems that could include singular interactions like r^{-1} (e.g., the Coulomb potential). However, the effective potential $U(r)$ will be treated numerically. Therefore, for meaningful results, it must be non-singular, bounded everywhere and, preferably but not necessarily, short range [9]. Now, the discrete L^2 bases used in the calculation and analysis are required to carry a tridiagonal matrix representation for the reference wave operator. The use of discrete basis sets offers considerable advantage in the calculation because it is an algebraic scheme that requires only standard matrix technique. The real power of our approach comes from the unique feature of J-matrix method that allowed us to isolate the r^{-1} singularity of the Yukawa potential and absorb it into the reference Hamiltonian where it is treated exactly analytically [10]. Moreover, the choice of basis, which supports a tridiagonal matrix representation for the reference wave operator, results in a very efficient, stable and highly accurate means for evaluating the matrix elements of the remaining regular part (the effective potential) using the Gauss quadrature integral approximation [11]. Broeckhove *et al* introduced modification to the J-matrix method to improve its convergence and reduce the computational cost [12]. They demonstrated their approach by application to the Yukawa potential with no special treatment of its singularity. The 'oscillator basis' was used and the reference Hamiltonian contained only the kinetic energy operator. In our approach, we use an alternative basis (the 'Laguerre basis') to comply with the J-matrix requirement of a tridiagonal matrix representation for the reference Hamiltonian that includes now the r^{-1} singularity. Working in a finite but highly accurate matrix representation of the total Hamiltonian, we study the bound states spectrum and resonance energies using the method of complex scaling [13]. We investigate the behavior of these energy eigenvalues and follow their trajectories in the complex energy plane as we vary the two Yukawa potential parameters. As a result, we confirm the observation that as the potential parameters vary, bound states move up the energy spectrum until they reach the continuum where they experience transition into scattering states[3]. The transition from a bound state with vanishing decay width to a resonance with finite lifetime in the continuum is referred to in the literature as the Mott transition [14]. This phenomenon is demonstrated graphically and shown as video animation. To illustrate the utility and accuracy of our approach, bound states and resonances energies are compared satisfactorily with those obtained by other studies. Additionally, we present results for a range of values of the potential parameters that were never probed before. In the following, we start

[3] The same observation has recently been reported in [6].

developing the tools of the approach and then apply them with the help of the J-matrix and complex scaling methods to arrive at our findings.

The time-independent Schrödinger equation for a particle of mass m and charge q in the combined field generated by the Coulomb potential and a spherically symmetric potential $V(r)$ reads as follows:

$$(H - E)|\psi\rangle = \left[-\frac{1}{2}\frac{\mathrm{d}^2}{\mathrm{d}r^2} + \frac{\ell(\ell+1)}{2r^2} + \frac{Z}{r} + V(r) - E\right]|\psi\rangle = 0, \tag{2}$$

where we have used the atomic units $\hbar = m = q = 1$ and length is measured in units of $a_0 = 4\pi\varepsilon_0\hbar^2/mq^2$. In our case, $V(r)$ is the Yukawa potential given by equation (1). The combination $\frac{Z}{r} + V(r)$ in equation (2) is a Hellmann-type potential. Because of the r^{-1}-type singularity of this potential, which is easily handled by the J-matrix method, we absorb it in the reference Hamiltonian by writing it as follows:

$$H_0 = -\frac{1}{2}\frac{\mathrm{d}^2}{\mathrm{d}r^2} + \frac{\ell(\ell+1)}{2r^2} + \frac{\mathcal{Z}}{r}, \tag{3}$$

where $\mathcal{Z} = Z - A$. Therefore, the effective potential $U = H - H_0$, which will be treated numerically, has the following form [15][4]:

$$U(r) = -\frac{A}{r}(\mathrm{e}^{-\mu r} - 1). \tag{4}$$

One can easily verify that this effective potential is regular and bounded everywhere. Consequently, we can evaluate its contribution (matrix elements) in a suitable L^2 basis to the desired accuracy using any preferred numerical integration scheme. The r^{-1}-type singularity in the reference Hamiltonian and the requirement that its matrix representation be tridiagonal dictate that the J-matrix basis used should be the 'Laguerre basis' defined as [10]

$$\phi_n(x) = a_n x^\alpha \,\mathrm{e}^{-x/2}\, L_n^\nu(x); \qquad n = 0, 1, 2, \ldots \tag{5}$$

where $x = \lambda r$, $\lambda > 0$, $\alpha > 0$, $\nu > -1$, $L_n^\nu(x)$ is the Laguerre polynomial and a_n is the normalization constant $\sqrt{\lambda\Gamma(n+1)/\Gamma(n+\nu+1)}$. Choosing $\alpha = \ell + 1$ and $\nu = 2\ell + 1$ gives the following tridiagonal matrix representation for H_0 [16]:

$$\frac{8}{\lambda^2}(H_0)_{nm} = \left(2n + \nu + 1 + \frac{8\mathcal{Z}}{\lambda}\right)\delta_{n,m} + \sqrt{n(n+\nu)}\,\delta_{n,m+1} + \sqrt{(n+1)(n+\nu+1)}\,\delta_{n,m-1}. \tag{6}$$

In the manipulation, we used the differential equation, differential formula, three-term recursion relation and orthogonality formula of the Laguerre polynomials [17]. Now, the only remaining quantity that is needed to perform the calculation is the matrix elements of the effective potential $U(r)$. This is obtained by evaluating the integral

$$U_{nm} = \int_0^\infty \phi_n(\lambda r)U(r)\phi_m(\lambda r)\,\mathrm{d}r = \lambda^{-1}a_n a_m \int_0^\infty x^\nu \,\mathrm{e}^{-x}\, L_n^\nu(x)L_m^\nu(x)[xU(x/\lambda)]\,\mathrm{d}x. \tag{7}$$

The evaluation of such an integral for a general effective potential is almost always done numerically. We use the Gauss quadrature approximation [11], which gives

$$U_{nm} \cong \sum_{k=0}^{N-1} \Lambda_{nk}\Lambda_{mk}[\varepsilon_k U(\varepsilon_k/\lambda)], \tag{8}$$

for adequately large integer N. ε_k and $\{\Lambda_{nk}\}_{n=0}^{N-1}$ are the N eigenvalues and corresponding eigenvectors of the $N \times N$ tridiagonal basis overlap matrix $\langle\phi_n \mid \phi_m\rangle$. Therefore, the reference Hamiltonian H_0 in this representation, which is given by equation (6), is accounted for in full.

[4] A similar perturbative approach to find the bound states analytically was adapted by Smith [15].

On the other hand, the effective potential U is approximated by its matrix elements in a subset of the basis. In this communication, we limit our investigation to the structure and dynamics of bound states and resonances and are contented with a finite-dimensional representation of the total Hamiltonian. It is worthwhile noting that for a one-particle effective Hamiltonian, like in this work, there is a larger degree of freedom in the choice of basis since it is constrained only by the potential. However, in a many-particle approach this freedom is constrained by other physical considerations. Having the additional Coulomb term in H_0 will not affect our computations which are done analytically as shown in the matrix elements given by equation (6) with an effective charge $\mathcal{Z} = Z - A$. Our choice $Z = 0$ is just for comparison purposes with other groups[5] [18, 19] who took $Z = 0$ in their computations. In fact, we did take $Z \neq 0$ in table 3 where we show the rate of convergence of our calculation with the basis size N. Nonetheless, the screened Coulomb potential describes adequately a single particle problem. Having an additional Coulomb term superposed with the Yukawa potential might be meaningful in describing the effective interaction in a many-body environment [20]. However, in a many-particle J-matrix approach the choice of basis will be more involved since it requires a many-cluster configuration for both entrance and exit channels [21].

Direct study of bound states and resonances is usually performed in the complex energy plane (E-plane). In such studies, these states are identified with the poles of the Green's function, which is defined formally in the E-plane as $G(E) = (H - E)^{-1}$. For systems with self-adjoint Hamiltonian, resonances are located in the lower half of the second sheet of the complex energy plane. These are bound-like states that are unstable and decay with a rate that increases with the (negative) value of the imaginary part of the resonance energy due to the factor $\mathrm{e}^{-\mathrm{i}Et}$ in the wavefunction. Sharp or 'shallow' resonances (those located below and close to the real energy axis in the E-plane) are more stable. They decay more slowly and are easier to obtain than broad or 'deep' resonances that are located below, but far from, the real energy axis. Consequently, interest is normally focused on resonances with an imaginary part that is smaller that the real part. Moreover, resonances are not confined only to the continuum sector. For certain potentials (e.g., $V = V_0 r^2 \mathrm{e}^{-r}$) these may also be found embedded between bound states, such that the real part of the resonance energy becomes negative [22]. In such cases, however, these states are typically the most unstable, with the negative imaginary part of the energy being the largest. One of the methods of investigation of resonances in the E-plane is the complex scaling (a.k.a. complex rotation) method [13]. In this method, the radial coordinate gets transformed as $r \to r\,\mathrm{e}^{\mathrm{i}\theta}$, where θ is a real angular parameter. The effect of this transformation on the pole structure of the Green's function consists of the following: (1) the discrete bound state spectrum that lies on the negative energy axis remains unchanged; (2) the branch cut (the discontinuity) along the real positive energy axis rotates clockwise by the angle 2θ; (3) resonances in the lower half of the complex energy plane located in the sector bound by the new rotated cut line and the positive energy axis get exposed and become isolated. However, due to the finite size of the basis used in the calculation, the rotated cut line gets replaced by a string of interleaved poles and zeros of the finite Green's function, which tries to mimic the cut structure. One can easily show that the complex scaling transformation $r \to r\,\mathrm{e}^{\mathrm{i}\theta}$ of the total Hamiltonian in configuration space is equivalent to the transformation of its matrix elements by changing the scale parameter as $\lambda \to \lambda\,\mathrm{e}^{-\mathrm{i}\theta}$.

Figure 1 is a snapshot from a video animation (a series of accurate graphical representations) in the E-plane of the calculated energy eigenvalues of the finite $N \times N$ total Hamiltonian matrix without complex scaling ($\theta = 0$). In the animation, we took $\ell = 1$,

[5] The variational energies of the bound states and resonances for $\ell = 1, 2, \ldots, 10$ were collected from Bylicki website http://www.fizyka.umk.pl/~mirekb/yukawa.html.

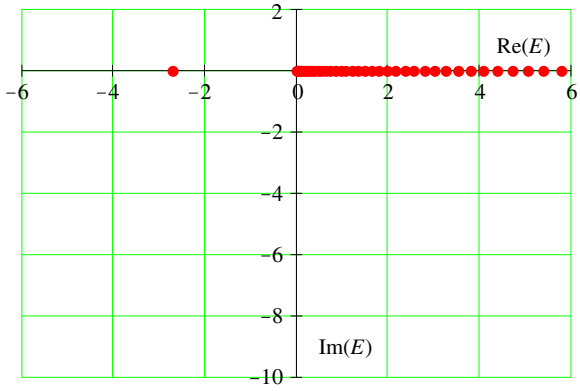

Figure 1. (1.26 MB MPG) Snapshot from video animation of the calculated energy eigenvalues of the finite total Hamiltonian matrix in the E-plane without complex scaling ($\theta = 0$). During the animation, A was varied from 80 to 0.0 (au) and we took $\ell = 1$, $\mu = 5$ (au).

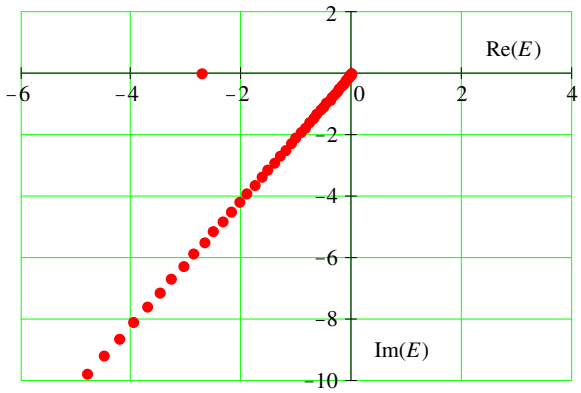

Figure 2. (1.56 MB MPG) Snapshot from the same video animation but with complex scaling where $\theta = 1.0$ radians.

$\mu = 5$ (au) and A was varied from 80 to 0 (au). The string of points on the positive real line is the set of energy eigenvalues corresponding to the discretized continuum line. In the beginning where $A = 80$ there is only one bound state in view with an energy near $E = -3.2$ (au). As the bottom of the effective potential well rises (with A decreasing) this energy eigenvalue starts shifting up in the spectrum by moving to the right until it gets 'absorbed' into the continuum. Decreasing A further, a new bound state comes into view from left moving to the right until it eventually becomes embedded into the continuum as well. This process continues. In the second animation, from which figure 2 is obtained as a snapshot, we show how bound states do not just get absorbed into the continuum but, in fact, experience a transition into scattering states [14]. To illustrate this, we use the complex scaling method described briefly above. It is obvious from the second video that the bound states energy eigenvalues that move to the right half of the E-plane do not rotate with the continuum line but follow their own resonance trajectories. These trajectories are stable against variations in all computational parameters (the rotation angle θ, basis scaling parameter λ, etc). Figure 3 is a plot of these trajectories for the three states contributing to the animation. We have also seen the same phenomenon

Table 1. Bound states and resonance energies for the Yukawa potential with the given parameters. The strength of the potential is normalized as $A = 1.0$. Our results are compared with those of others [18, 19] (see footnote 5). All values are in atomic units.

References	ℓ	μ	E [references]	E [this work]
[18]	0	0.10	$-0.407\,058\,030\,613\,403\,156\,754\,507\,070$	$-0.407\,058\,030\,613$
		0.10	$-0.049\,928\,271\,331\,918\,889\,234\,996\,681$	$-0.049\,928\,271\,332$
	1	0.200 00	$-4.101\,646\,530\,7840 \times 10^{-3}$	$-4.101\,646\,530\,802 \times 10^{-3}$
	2	0.08	$-3.248\,360\,428\,751\,9935 \times 10^{-3}$	$-3.248\,360\,428\,763 \times 10^{-3}$
[19]	1	0.112	$-5.003\,810 \times 10^{-5}$	$-5.008\,834\,873\,206 \times 10^{-5}$
		0.113	$+1.631\,328 \times 10^{-5} - \mathrm{i}\,1.0250 \times 10^{-6}$	$+1.690\,357\,641\,732 \times 10^{-5} - \mathrm{i}\,1.862\,588\,128\,150 \times 10^{-6}$
		0.122	$+4.216\,372\,95 \times 10^{-4} - \mathrm{i}\,3.251\,9395 \times 10^{-4}$	$+4.214\,837\,407\,095 \times 10^{-4} - \mathrm{i}\,3.251\,672\,270\,506 \times 10^{-4}$
See footnote 5	1	0.112 604 85	$-3.932\,6971 \times 10^{-2}$	$-3.932\,698\,311\,615 \times 10^{-2}$
		0.113 240 71	$+3.096\,4751 \times 10^{-5} - \mathrm{i}\,4.628\,3598 \times 10^{-6}$	$+3.096\,253\,670\,542 \times 10^{-5} - \mathrm{i}\,4.640\,977\,622\,365 \times 10^{-6}$
		0.221 317 05	$+1.375\,8648 \times 10^{-4} - \mathrm{i}\,1.528\,7316 \times 10^{-5}$	$+1.375\,843\,424\,574 \times 10^{-4} - \mathrm{i}\,1.528\,916\,191\,194 \times 10^{-5}$
	2	0.092	$+1.410\,647 \times 10^{-4} - \mathrm{i}\,1.1700 \times 10^{-6}$	$+1.410\,607\,617\,484 \times 10^{-4} - \mathrm{i}\,1.170\,284\,982\,249 \times 10^{-6}$
		0.207 193 91	$-7.434\,4785 \times 10^{-3}$	$-7.434\,478\,537\,514 \times 10^{-3}$
		0.207 193 91	$+7.561\,4845 \times 10^{-4} - \mathrm{i}\,5.3974260 \times 10^{-4}$	$+7.561\,484\,464\,990 \times 10^{-4} - \mathrm{i}\,5.397\,425\,935\,464 \times 10^{-4}$
	5	0.324 319 43	$+2.879\,1297 \times 10^{-5} - \mathrm{i}\,4.908\,1260 \times 10^{-12}$	$+2.879\,132\,724\,089 \times 10^{-5} - \mathrm{i}\,4.651\,948\,920\,811 \times 10^{-12}$
		0.392 665 64	$+9.497\,8169 \times 10^{-4} - \mathrm{i}\,2.449\,7104 \times 10^{-4}$	$+9.497\,816\,886\,083 \times 10^{-4} - \mathrm{i}\,2.449\,710\,308\,446 \times 10^{-4}$
	10	0.342 834 28	$-5.556\,3066 \times 10^{-6}$	$-5.556\,304\,541\,175 \times 10^{-6}$
		0.344 955 66	$+7.218\,8283 \times 10^{-6} - \mathrm{i}\,0.000$	$+7.218\,866\,481\,722 \times 10^{-6} - \mathrm{i}\,1.786\,030\,250\,706 \times 10^{-15}$

Table 2. Bound states and resonance energies for a wider range of parameters of the Yukawa potential. All values are in atomic units.

	ℓ	μ	A	E
Bound states	0	1.0	30	−420.734 052 0442
				−85.294 720 788 85
				−25.849 431 442 98
				−7.656 289 423 403
				−1.517 703 985 470
				−0.020 763 186 246
	1	0.5	20	−40.596 985 428 31
				−13.631 564 171 58
				−4.917 728 174 528
				−1.546 320 478 514
				−0.285 657 326 503
	2	0.2	10	−3.751 512 770 069
				−1.494 005 746 764
				−0.566 900 519 026
				−0.168 517 340 167
				−0.019 233 342 003
Resonances	2	10	108	3.060 697 264 14 − i 0.062 214 727 55
			170	2.484 957 438 98 − i 0.080 496 968 75
			248	1.502 758 9904 − i 0.037 679 6110
	5	2	110	2.420 889 9272 − i 0.076 858 9832
				3.013 948 8985 − i 3.604 952 7387
			170	1.024 443 520 − i 0.003 598 625
				2.236 370 014 − i 2.381 751 848
			200	1.359 477 152 − i 0.029 358 570
				1.815 292 940 − i 2.549 254 736
	10	1	200	1.057 885 231 − i 0.000 001 090
				1.651 827 352 − i 4.794 059 401
				3.065 622 630 − i 2.731 016 510
				3.264 518 294 − i 0.639 296 036

repeated when fixing the strength of the potential A while varying its range parameter μ. Video animations and figures for this case are available upon request from the corresponding author.

To illustrate further the utility and accuracy of our approach, we use it to calculate bound states and resonance energies for a given set of physical parameters where we can compare our results with those obtained elsewhere [18, 19] (see footnote 5). Our calculation strategy is as follows. For a given choice of physical parameters, we investigate the stability of calculated eigenvalues that correspond to bound states and/or resonances as we vary the scaling parameter λ until we reach a plateau in λ [23]. Then to improve on the accuracy of the results, we select a value of λ from within the plateau and increase the dimension of the space N until the desired accuracy is reached. Table 1 lists some of the bound states and resonance energies where our results are compared with available numerical data [18, 19] (see footnote 5) satisfactorily. However, table 2 contains results that are unique to our approach since the values of the potential parameters and range of energies fall outside the applicability

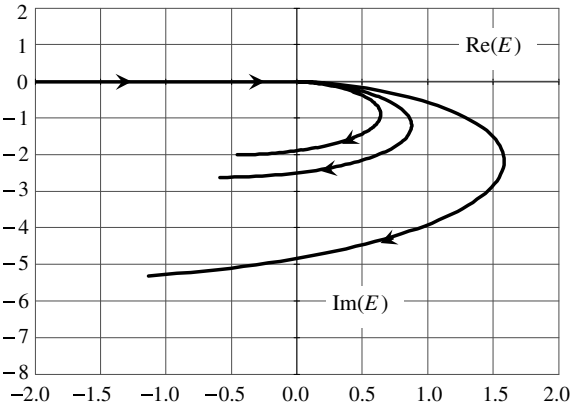

Figure 3. A plot in the complex energy plane of the trajectories of the energy eigenvalues (in atomic units) corresponding to the three states (bound and resonance) contributing to the video animation.

Table 3. Rate of convergence of our calculation with the basis size N. We list bound states energies for a given set of physical parameters (all in atomic units). We took a non-zero Coulomb charge ($Z = 5$ for all). For the set of results with $\mu = 0.2$ and $\mu = 0.5$, we took $A = 15$ and $\ell = 1$. However, for $\mu = 0.7$ and $\mu = 1.0$, we took $A = 20$ and $\ell = 0$.

μ	$N = 5$	$N = 10$	$N = 15$	$N = 30$	$N = 50$
0.2	9.614 261 235 426	9.644 658 116 717	9.644 664 974 192	9.644 664 974 936	9.644 664 974 935 78
	2.900 686 172 717	2.901 595 170 495	2.901 595 172 998	2.901 595 172 998	2.901 595 172 998 09
	0.729 583 582 889	0.729 834 164 058	0.729 834 165 016	0.729 834 165 016	0.729 834 165 016 40
0.5	5.840 256 925 186	5.866 288 283 420	5.866 300 243 571	5.866 300 248 314	5.866 300 248 313 82
	0.054 831 962 128	0.056 313 117 618	0.056 313 222 725	0.056 313 222 746	0.056 313 222 745 99
0.7	96.197 054 383 58	98.963 536 611 46	98.975 782 492 98	98.975 811 483 42	98.975 811 483 4149
	15.892 592 137 35	15.910 877 340 77	15.910 877 617 79	15.910 877 617 80	15.910 877 617 7983
	2.189 033 498 853	2.192 676 846 601	2.192 676 961 610	2.192 676 961 613	2.192 676 961 613 25
1.0	90.725 018 836 43	93.447 371 131 65	93.459 768 680 42	93.459 800 369 88	93.459 800 369 8851
	11.632 898 234 10	11.652 905 490 99	11.652 906 403 25	11.652 906 403 31	11.652 906 403 3084

of most perturbative and variational calculations found elsewhere. For the two tables, we took the basis size $N = 200$. Table 3 shows the convergence rate of our calculation of bound states energy spectrum with the basis size N for a given set of physical parameters. However, the larger the size of the spectrum, the larger the value of N needed to maintain the same accuracy over the whole spectrum. More results could also be obtained from the corresponding author. Finally, this approach could easily be generalized to handle other short-range potentials with r^{-1} singularity. For example, we are currently involved in extending it to the Hulthén potential.

Acknowledgments

The authors acknowledge the support provided by the Physics Department at King Fahd University of Petroleum & Minerals.

References

[1] Yukawa H 1935 *Proc. Phys. Math. Soc. Japan* **17** 48
[2] Wilczek Frank 2007 *Nature* **445** 156
[3] Siemens P J 1970 *Phys. Rev.* C **1** 98
Lee S J, Gan H H, Cooper E D and Das Gupta S 1989 *Phys. Rev.* C **40** 2585
[4] Kar S and Ho Y K 2007 *Phys. Rev.* A **75** 062509
[5] Messina R and Lowen H 2003 *Phys. Rev. Lett.* **91** 146101
[6] Bylicki M, Stachów A, Karwowski J and Mukherjee P K 2007 *Chem. Phys.* **331** 346
[7] Gomes O A, Chacham H and Mohallem J R 1994 *Phys. Rev.* **50** 228 and references therein
[8] Heller E J and Yamani H A 1974 *Phys. Rev.* A **9** 1201
Heller E J and Yamani H A 1974 *Phys. Rev.* A **9** 1209
[9] Vanroose W, Broeckhove J and Arickx F 2001 *Phys. Rev. Lett.* **88** 010404
[10] Yamani H A and Fishman L 1975 *J. Math. Phys.* **16** 410
[11] See, for example, Appendix A in: Alhaidari A D, Yamani H A and Abdelmonem M S 2001 *Phys. Rev.* A **63** 062708
[12] Broeckhove J, Arickx F, Vanroose W and Vasilevsky V S 2004 *J. Phys. A: Math. Gen.* **37** 7769
[13] Aguilar J and Combes J M 1971 *Commun. Math. Phys.* **22** 269
Ho Y K 1983 *Phys. Rep.* **99** 1
[14] Blaschke D, Burau G, Kalinovsky Yu and Barnes T 2003 *Eur. Phys. J.* A **18** 547
Redmer R 1997 *Phys. Rep.* **282** 35
[15] Smith C R 1964 *Phys. Rev.* **134** A1235
[16] Alhaidari A D 2005 *Ann. Phys.* **317** 152
[17] Magnus W, Oberhettinger F and Soni R P 1966 *Formulas and Theorems for the Special Functions of Mathematical Physics* 3rd edn (New York: Springer) pp 239–49
[18] Stubbins C 1993 *Phys. Rev.* A **48** 220
[19] Haberland H, Kraeft W, Schlanges M and Gericke D O 1995 *Physica* A **220** 618
[20] Ikhdair S M and Sever R 2007 *J. Math. Chem.* **41** 343
[21] Vasilevsky V, Nesterov A V, Arickx F and Broeckhove J 2001 *Phys. Rev.* C **63** 064604
Zaitsev S A, Smirnov Yu F and Shirokov A M 1998 *Theor. Math. Phys.* **117** 1291
[22] Engdahl E, Brändas E, Rittby M and Elander N 1988 *Phys. Rev.* A **37** 3777
Alhaidari A D 2004 *J. Phys. A: Math. Gen.* **37** 5863
Rakityansky S A, Sofianos S A and Elander N 2007 *J. Phys. A: Math. Theor.* **40** 14857
[23] Nasser I M, Abdelmonem M S, Bahlouli H and Alhaidari A D 2007 *J. Phys. B: At. Mol. Opt. Phys.* **40** 4245